

General Disclaimer

One or more of the Following Statements may affect this Document

- This document has been reproduced from the best copy furnished by the organizational source. It is being released in the interest of making available as much information as possible.
- This document may contain data, which exceeds the sheet parameters. It was furnished in this condition by the organizational source and is the best copy available.
- This document may contain tone-on-tone or color graphs, charts and/or pictures, which have been reproduced in black and white.
- This document is paginated as submitted by the original source.
- Portions of this document are not fully legible due to the historical nature of some of the material. However, it is the best reproduction available from the original submission.

X-921-77-259

PREPRINT

TM-78054
**OCEAN GRAVITY AND
GEOID DETERMINATION**

(NASA-TM-78054) OCEAN GRAVITY AND GEOID
DETERMINATION (NASA) 25 p HC A02/MP A01
CSCL 08N

N78-13672

G3/46 Unclass
55997

**W. D. KAHN
J. W. SIRY
R. D. BROWN
W. T. WELLS**

OCTOBER 1977



**GODDARD SPACE FLIGHT CENTER
GREENBELT, MARYLAND**

X-921-77-259
PREPRINT

OCEAN GRAVITY AND
GEOID DETERMINATION

W. D. Kahn
J. W. Siry
Goddard Space Flight Center

R. D. Brown
Computer Sciences Corp.
Silver Spring, Maryland

W. T. Wells
EG&G/Washington Analytical Services, Inc.
Riverdale, Maryland

October 1977

GODDARD SPACE FLIGHT CENTER
Greenbelt, Maryland

OCEAN GRAVITY AND
GEOID DETERMINATION

W. D. Kahn
J. W. Siry
Goddard Space Flight Center

R. D. Brown
Computer Sciences Corp.
Silver Spring, Maryland

W. T. Wells
EG&G/Washington Analytical Services, Inc.
Riverdale, Maryland

ABSTRACT

Gravity anomalies have been recovered in the North Atlantic and the Indian Ocean regions. Comparisons of 63 $2^\circ \times 2^\circ$ mean free air gravity anomalies recovered in the North Atlantic area and 24 $5^\circ \times 5^\circ$ mean free air gravity anomalies in the Indian Ocean area with surface gravimetric measurements have shown agreement to ± 8 mgals for both solutions. Geoids derived from the altimeter solutions are consistent with altimetric sea surface height data to within the precision of the data, about ± 2 meters.

CONTENTS

| | <u>Page</u> |
|---|-------------|
| INTRODUCTION | 1 |
| MEASUREMENT GEOMETRY AND MATHEMATICAL MODELS..... | 2 |
| RESULTS | 8 |
| CONCLUSION | 15 |
| REFERENCES..... | 20 |

ILLUSTRATIONS

| <u>Figure</u> | | <u>Page</u> |
|---------------|---|-------------|
| 1 | Altimeter Measurement Geometry | 2 |
| 2 | $2^{\circ} \times 2^{\circ}$ Mean Free Air Gravity Anomaly Recovery Solution..... | 10 |
| 3 | Differences Between Estimated $2^{\circ} \times 2^{\circ}$ Gravity Anomalies and Ground Truth | 11 |
| 4 | Comparison of GEOS-3 Altimeter Geoid with Detailed Geoid and Altimeter Sea Surface Height Profile for Revolution 1647 ... | 13 |
| 5 | $5^{\circ} \times 5^{\circ}$ Gravity Anomalies Recovered from GEOS-3 Altimetry Data and Apollo/Soyuz SST Data in the East Indian Ocean Area | 14 |
| 6 | Comparison of GEOS-3 Altimeter Geoid with the Detailed Geoid and Sea Surface Height Profile for Revolution 1383..... | 15 |
| 7 | Comparison of GEOS-3 Altimeter Geoid with the Detailed Geoid and Sea Surface Height Profile for Revolution 1710..... | 16 |
| 8 | Comparison of GEOS-3 Altimeter Geoid with the Detailed Geoid and Sea Surface Height Profile for Revolution 1661..... | 17 |

ILLUSTRATIONS (Continued)

| <u>Figure</u> | | <u>Page</u> |
|---------------|--|-------------|
| 9 | Comparison of GEOS-3 Altimeter Geoid with the Detailed Geoid and Sea Surface Height Profile for Revolution 1718..... | 18 |
| 10 | East Indian Ocean Area | 19 |

OCEAN GRAVITY AND GEOID DETERMINATION

INTRODUCTION

A spacecraft borne altimeter measures the height of the spacecraft above the instantaneous sea surface. In general, this surface deviates from the mean sea surface by no more than a few meters. The equipotential surface that corresponds to the mean sea surface (in the absence of dynamic effects such as ocean tides, currents, surges, etc.) is called the geoid. Since altimeter measurements are made relative to the instantaneous sea surface which closely follows the geoid, the altimeter measurements offer the best possibility for improving the accuracy of the marine geoid, and, by inversion, the marine gravity field.

The GEOS-3 altimeter has demonstrated the capability to measure the fine structure of the mean sea surface. When this instrument is operating in the short pulse mode, a measurement is produced every 4 km footprint along the satellite subtrack. With this resolution capability it will be possible to describe sea surface topography to a detail of less than 1° , depending on the degree of data smoothing used and the spacing between subtracks. The data from the GEOS-3 altimeter constitutes an in-situ set of measurements of the sea surface, providing independent data over areas where surface measurements exist, and filling gaps in those regions of the sea surface where surface measurements are sparse or non-existent.

In this investigation, emphasis is placed on the recovery of gravity anomalies from altimetry data in the N. Atlantic region bounded by latitude 20°N to 40°N and longitude 280°E to 300°E and the Indian Ocean area bounded by latitude 20°S to 50°S and longitude 90°E to 110°E . The recovered gravity anomalies are compared with gravity anomalies derived from surface gravity data only in the Atlantic area and with both surface gravity data and Apollo-Soyuz (Ref. 1) geodynamics experiment recovered values for gravity anomalies in the Indian Ocean area. In addition, intercomparisons between recovered geoid, and altimeter sea surface height and the $1^\circ \times 1^\circ$ detailed geoid are studied for representative altimeter passes in the Atlantic and Indian Ocean areas.

The GEOS-3 altimetry data used in the solution for the North Atlantic region consisted of over 35,000 well distributed altimeter measurements obtained from portions of 80 altimeter passes which traversed the area. For the Indian Ocean area approximately 7200 well distributed GEOS-3 altimeter measurements were selected from over 72,000 measurements in 31 passes which traversed that area.

MEASUREMENT GEOMETRY AND MATHEMATICAL MODELS

The geometry associated with the altimeter measurement is described in Figure 1. As can be seen, the altimeter is nominally the shortest distance between the satellite and the sea surface, that is, the measurement is along the normal to the sea surface that passes through the satellite.

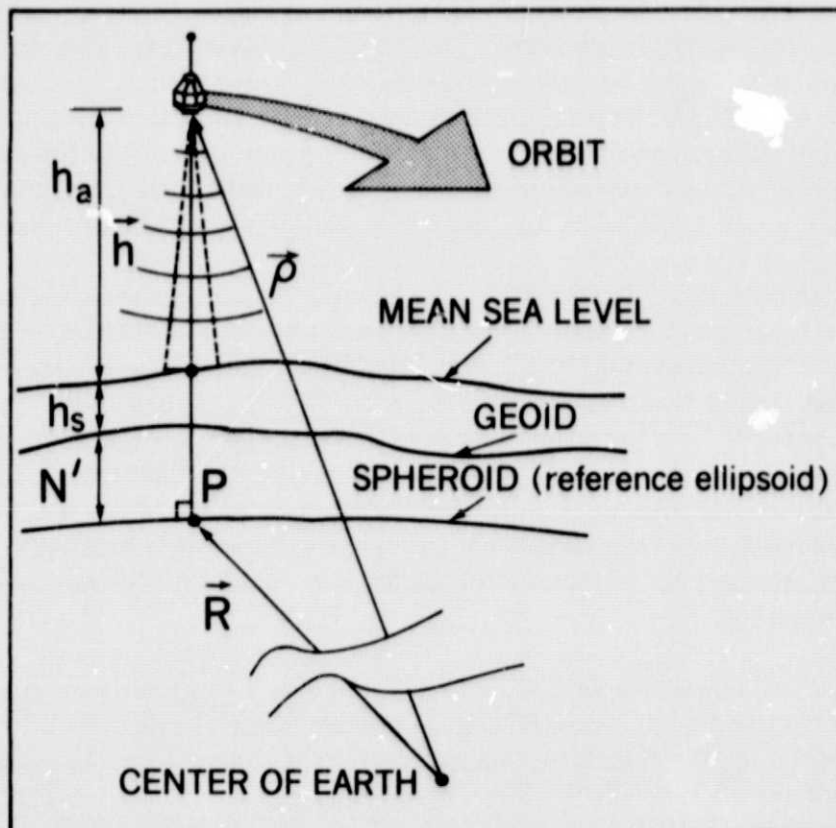


Figure 1. Altimeter Measurement Geometry

The mathematical model for the altimeter measurement is given by the following relationship

$$h_a = h - N' - h_s - \Delta h' \quad (1)$$

where

$$h_a = \text{S/C altitude above sea surface}$$

- h = magnitude of \vec{h} , the height of the spacecraft above the reference ellipsoid
 N' = geoid height above reference ellipsoid
 h_s = deviation of sea surface from geoid
 $\Delta h'$ = systematic errors in altimeter measurement, e.g., refraction, antenna offset, timing, etc.

The high rate (10/sec or 100/sec) binary format altimeter measurement data are processed in the GEODYN Program, (a general purpose orbit determination program which is used at the NASA Goddard Space Flight Center, where a tidal correction is applied and the data are converted to geoid heights and fit to a reference geopotential level surface. The tidal correction model in GEODYN includes corrections for both ocean tides (Hendershott model) and solid earth tides (Ref. 2), but only the M2 component is considered. The GEODYN Program has been modified to permit the differential correction of orbital elements from altimeter data. This process can be used to converge the altimetric geoid heights to a profile through a reference geopotential level surface, in this case, the GEM-7 geoid (Ref. 3). The corrected orbit parameters serve merely as accommodation coefficients in this process and effect a removal of bias, trend, and long wavelength curvature from the relatively short arcs of altimeter data. While all six orbit parameters are adjusted, significant changes (greater than the standard deviation of the estimate) usually only occur in the orbit semi major axis, eccentricity and the true anomaly. Insignificant changes in the remaining Keplerian parameters may also occur for the longer arcs.

This process minimizes the square of deviation of the altimetric geoid heights from the GEM 7 geoid.

To model the geoid surface, one must describe the gravitational potential. This is usually done in terms of the potential of the reference ellipsoid, the normal potential, and the disturbing potential. The disturbing potential at the point $P(\phi, \lambda, r)$ is expressed in terms of spherical harmonics as follows:

$$T = \frac{GM}{r} \sum_{n=2}^L \left(\frac{a}{r}\right)^n \sum_{m=0}^n P_{nm}(\sin \phi) [C_{nm} \cos m\lambda + S_{nm} \sin m\lambda] \quad (2)$$

where

GM = gravitational constant of the earth

C_{nm}, S_{nm} = spherical harmonic expansion coefficients

$P_{nm}(\sin \phi)$ = associated Legendre functions

(ϕ, λ) = latitude and longitude at which disturbing potential is evaluated

r = geocentric radius from earth center of mass to evaluation point P

a = semi-major axis of reference ellipsoid

L = is the limit of summation, and it is specified by the degree of harmonic expansion of the global geoid

n = summation index for degree terms of the spherical harmonic expansion of T

m = summation index for the order of terms in spherical harmonic expansion of T

The geoid height at point P is expressed by

$$N' = N_1 + \Delta N_1 \quad (3)$$

where

$N_1 = \frac{T}{\gamma}$ (Bruns' Formula Ref. 4), the global geoid model undulation

γ = magnitude of gravity vector normal to reference ellipsoid

ΔN_1 = a local correction to the global geoid model values

The global model contribution to the geoidal undulation at any point P (ϕ, λ, r) on the geoid can be computed from geopotential coefficients derived from satellites by analysis of perturbations on the orbits induced by the Earth's gravity field.

The Stokes' formula (Ref. 4, pp. 92-98) is another form of expressing the disturbing potential. This formula makes it possible to express the local details of the disturbing potential in terms of gravity data. That is,

$$T = \frac{R}{4\pi} \int \int \Delta g S(\psi) d\sigma \quad (4)$$

where

$$R = a(1 - f)^{1/3}$$

is the mean spherical radius of the earth,

f = flattening of reference ellipsoid

S(ψ) = Stokes' function

σ = element of area

Δg = surface gravity anomalies

$$S(\psi) = \csc\left(\frac{\psi}{2}\right) - 6 \sin \frac{\psi}{2} + 1 - 6 \cos \psi - 3 \cos \psi \ln \left(\sin \frac{\psi}{2} + \sin^2 \frac{\psi}{2} \right) \quad (5)$$

From Bruns' formula the geoidal undulation at any point P on the geoid can be computed from Stokes' formula (Equation 4). That is;

$$N = \frac{T}{\gamma} = \frac{R}{4\pi\gamma} \iint_{\sigma} \Delta g S(\psi) d\sigma \quad (6)$$

In terms of geographical coordinates, Stokes' function can be expressed as follows:

$$N(\phi, \lambda) = \frac{R}{4\pi\gamma} \int_{\lambda'=0}^{2\pi} \int_{\phi'=-\pi/2}^{\pi/2} \Delta g(\phi', \lambda') S(\psi) \cos \phi' d\phi' d\lambda' \quad (7)$$

where

$$d\sigma = \cos \phi' d\phi' d\lambda'$$

(ϕ, λ) = latitude and longitude of the computation point

(ϕ', λ') = coordinates of the variable surface element σ

ψ = spherical distance between the computation point and variable surface element

$$\psi = \cos^{-1} [\sin \phi \sin \phi' + \cos \phi \cos \phi' \cos (\lambda - \lambda')]$$

$\Delta g(\phi' \lambda')$ = free-air gravity anomaly at the variable point $(\phi' \lambda')$

γ = mean value of gravity over Earth

To combine surface gravity data and geopotential information derived from gravity field perturbations acting on orbits of spacecraft, the Earth is divided into two areas (Ref. 3), a global area (A_1) and a local area (A_2), surrounding the point P. Each gravity anomaly in each area is also partitioned into two parts represented by Δg_s and Δg_2 respectively, where the global model contribution, Δg_s is given by

$$\Delta g_s = \gamma \left[\sum_{n=2}^L \sum_{m=0}^n (n-1) \left(\frac{a}{r}\right)^n P_{nm}(\sin \phi) \{C_{nm} \cos n\lambda + S_{nm} \sin m\lambda\} \right] \quad (8)$$

The Δg_2 value is defined as the local gravity anomaly. By partitioning the geoidal undulations into two corresponding components, Equation 7 can therefore be rewritten as follows:

$$N(\phi, \lambda) = N_1 + \Delta N_1 \quad (9)$$

where

$$N_1 = \frac{R}{4\pi\gamma} \int_0^{2\pi} \int_{-\pi/2}^{\pi/2} \Delta g_s(\phi', \lambda') S(\psi) \cos \phi' d\phi' d\lambda'$$

is the global model undulation term

and

$$\Delta N_1 = \frac{R}{4\pi\gamma} \int_{\Lambda_2} \int \Delta g_2(\phi', \lambda') S(\psi) \cos \phi' d\phi' d\lambda'$$

is the local undulation. Note that this partitioning also implies a partitioning in the disturbing potential. If we define

$$\Delta N_1 = \frac{\Delta T}{\gamma}$$

and

$$\Delta g_2 = \delta(\Delta g_s)$$

then

$$N(\phi, \lambda) = \frac{T + \Delta T}{\gamma} \quad (10)$$

or

$$N = N_1 + \frac{R \Delta \phi' \Delta \lambda'}{4\pi\gamma} \sum_{j=1}^{\bar{L}} \delta \left\{ \Delta g_s(\phi'_j, \lambda'_j) \right\} S(\psi_j) \cos \phi'_j$$

where ΔN_1 is the correction to the geoidal undulations of the global geoid as a function of the corrections of mean free air gravity anomalies.

Equation 10 is the form of the parameterization adopted for relating the altimeter measurement residuals to geoidal parameters. That is by defining

$$\delta \tilde{N} = \Delta h_a = \Delta N_1$$

$$\delta \tilde{g} = \delta \left\{ \Delta g_s(\phi'_j, \lambda'_j) \right\} \quad (11)$$

$$A = \frac{R \Delta \phi' \Delta \lambda'}{4\pi\gamma} S(\psi_j) \cos \phi'_j$$

Equation 10 is written in linear matrix form as follows:

$$\delta \tilde{N}_{(k \times 1)} = A_{(k \times j)} \delta \tilde{g}_{(j \times 1)} \quad (12)$$

where

$$j = 1, 2, 3, \dots, m$$

$$k \gg j$$

The gravity anomalies are estimated from altimetry data by using the weighted least squares estimation process. The solution vector $\delta \tilde{\mathbf{g}}_{(j \times 1)}$ of Equation 12 is obtained by solving Equation 13 below.

$$(\delta \tilde{\mathbf{g}})_{(j \times 1)} \approx \left[\sum_{\ell=1}^k (\mathbf{A}^T \mathbf{W}^{-1} \mathbf{A})_{\ell} + \mathbf{W}_{\delta \tilde{\mathbf{g}}_0}^{-1} \right]_{(j \times j)}^{-1} \left[\sum_{\ell=1}^k (\mathbf{A}^T \mathbf{W}^{-1} \delta \tilde{\mathbf{N}})_{\ell} + \mathbf{W}_{\delta \tilde{\mathbf{g}}_0}^{-1} \delta \tilde{\mathbf{g}}_0 \right]_{(j \times 1)} \quad (13)$$

where

\mathbf{W}^{-1} = weighting matrix of altimeter measurement.

$\mathbf{W}_{\delta \tilde{\mathbf{g}}_0}^{-1}$ = a priori covariance matrix for anomaly blocks to be estimated.

$\delta \tilde{\mathbf{g}}_0$ = initial estimate to solution vector.

The total gravity anomaly is computed by summing the local anomaly as obtained from (13) with the global contribution given by (9). That is:

$$\Delta \mathbf{g} = \Delta \mathbf{g}_s(\phi, \lambda) + \delta \tilde{\mathbf{g}} \quad (14)$$

where

$$\delta \tilde{\mathbf{g}} = \delta \{ \Delta \mathbf{g}_s(\phi, \lambda) \}$$

RESULTS

Area mean free air gravity anomaly solutions from altimetry data have been generated in the western North Atlantic and in the eastern Indian Ocean, west of Australia. Two degree by two degree equi-angular area means were estimated in the North Atlantic and $5^\circ \times 5^\circ$ area means for the eastern Indian Ocean

area. Each solution used the Goddard Earth Model-7 (GEM-7) geopotential model for starting anomaly values. In each solution, the resulting geoid surface fits the altimetric sea surface height observations closely, at or near the noise level associated with the altimeter data. This noise level, which varies with the changes in altimeter operating mode and sea surface phenomena, has been estimated by Brown (Ref. 5) at between 1.8 and 2.1 meters for data in the North Atlantic.

The quality of these solutions is difficult to measure since no accurate standard is yet in existence. Solution quality certainly varies from block to block, since the altimeter data density varies from block to block by one to two orders of magnitude. Aside from measures of self consistency (the fit of the solution geoid to the altimetric sea height data) the best test is to compare with other area mean free air gravity solutions. These other solutions are of two types: "ground truth" derived from point surface observations of gravity and independent solutions based on satellite to satellite tracking such as that obtained from the Apollo-Soyuz Geodynamics Experiment which used a different data type, and a different data processing technique than that described herein.

Figure 2(a) shows the tabulation of 63 estimated $2^\circ \times 2^\circ$ mean free air gravity anomalies in the Atlantic area and corresponding "ground truth" values based on $1^\circ \times 1^\circ$ surface gravity measurements compiled by the Defense Mapping Agency, Aerospace Center (DMAAC). The recovery region is bounded by latitudes 20°N to 40°N and longitudes 280°E to 300°E . For the solution, over 35,000 altimeter observations from approximately 80 passes over the recovery region were processed while the altimeter was operating in the short pulse mode. Figure 2(b) shows the recovery region and the distribution of altimeter passes over that region.

Differences between "ground truth" and estimated anomalies for a $10^\circ \times 10^\circ$ subblock solution are shown in Figure 3(a). Figure 3(b) shows the distribution of altimeter passes within this subblock area.

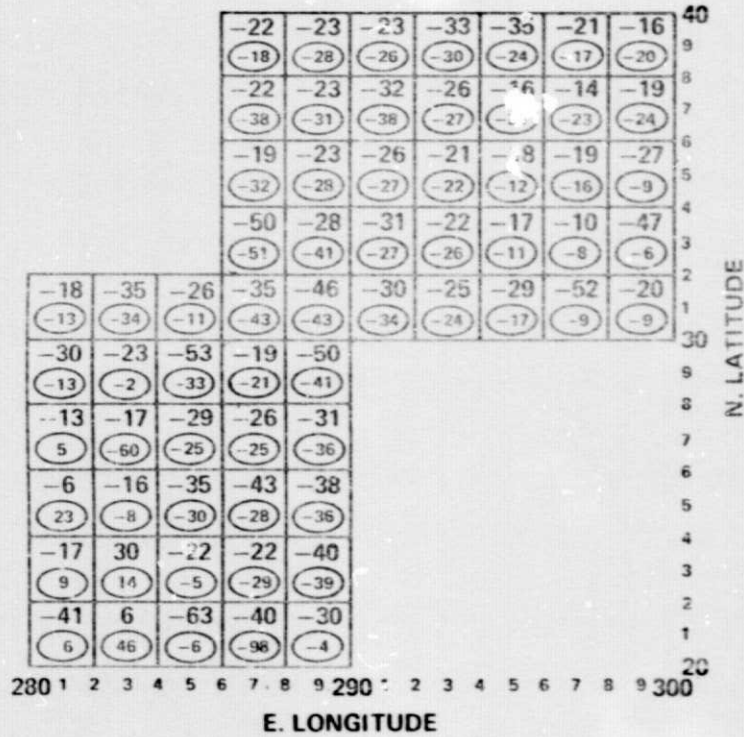
Note in Figure 3(a), that large anomaly differences result for area blocks 10 and 22 which have the worst distribution of altimeter data and also are the largest in magnitude from the other anomaly differences. Upon their deletion, the RMS error is reduced from 12.4 mgals to 6.4 mgals.

The accuracy of the $2^\circ \times 2^\circ$ gravity anomaly solution was checked by

- a) Computing a detailed gravimetric geoid using the 63 estimated $2^\circ \times 2^\circ$ mean free air gravity anomalies
- and

**ORIGINAL PAGE IS
OF POOR QUALITY**

(a) $2^\circ \times 2^\circ$ ANOMALIES AND "GROUND TRUTH"
(MILLIGALS)



RMS DEVIATION FROM GROUND TRUTH: ± 9.6 MGAL

LEGEND: ○ GROUND TRUTH: DMAAC
 SPHERICAL DIST. (ψ): 10°
 REFERENCE GRAVITY FIELD: GEM-7

(b) GROUND TRACKS
OF GEOS-3 ALTIMETER PASSES USED
IN SOLUTION

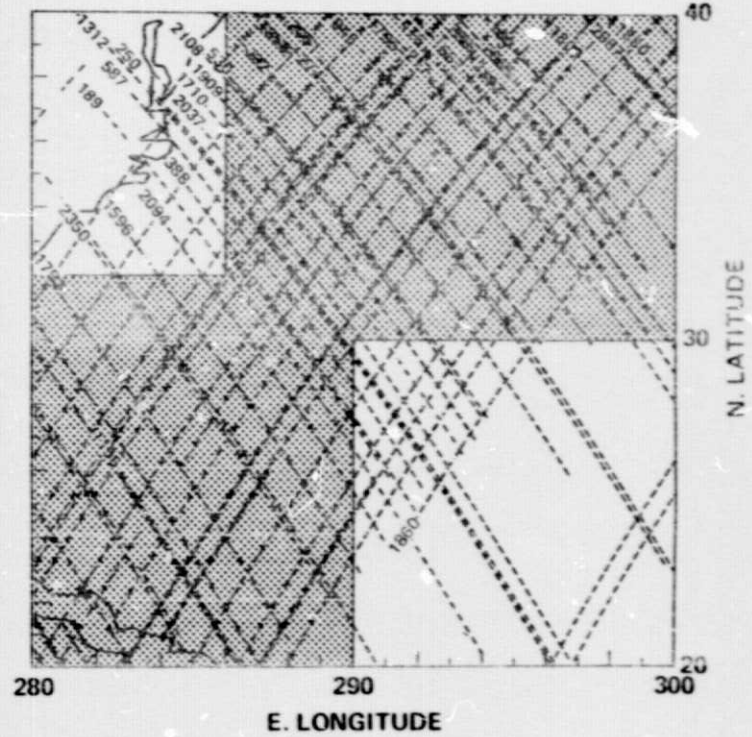


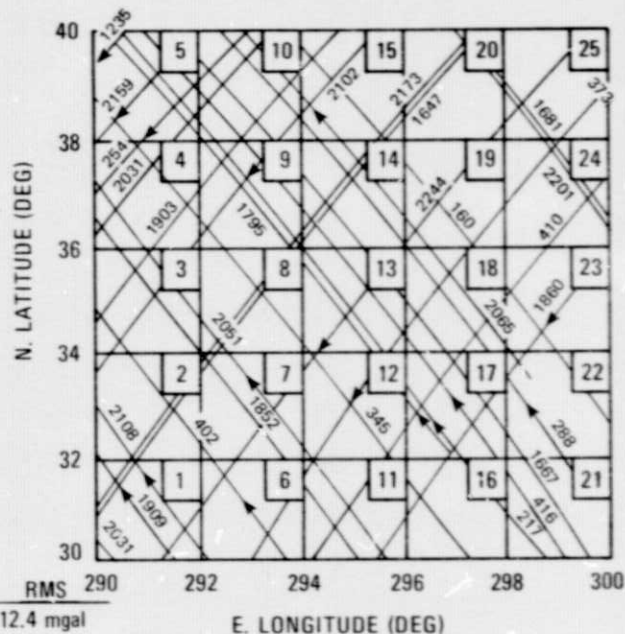
Figure 2. $2^\circ \times 2^\circ$ Mean Free Air Gravity Anomaly Recovery Solution

ORIGINAL PAGE IS
OF POOR QUALITY

(a) ANOMALY DIFFERENCES
(MILLIGALS)

| | | | | |
|------|------|-------|-------|-------|
| 5 | 10 | 15 | 20 | 25 |
| 3.5 | 0.2 | -14.6 | -5.0 | 0.8 |
| 4 | 9 | 14 | 19 | 24 |
| -4.7 | 6.6 | 5.3 | 10.0 | 2.2 |
| 3 | 8 | 13 | 18 | 23 |
| -4.2 | 2.0 | -6.2 | -2.6 | -13.0 |
| 2 | 7 | 12 | 17 | 22 |
| -7.7 | 4.1 | -5.2 | -2.4 | -41.0 |
| 1 | 6 | 11 | 16 | 21 |
| 0.2 | -0.9 | -15.1 | -43.0 | -11.0 |

(b) GROUND TRACKS OF
GEOS-3 ALTIMETER PASSES USED IN SOLUTION



| | MEAN | RMS |
|--|-----------|-------------|
| ANOMALY DIFFERENCES ALL BLOCKS | -5.6 mgal | ± 12.4 mgal |
| ANOMALY DIFFERENCES EXCL BLOCKS (16 & 22): | -2.4 mgal | ± 6.4 mgal |

- SPHERICAL DISTANCE (ψ) USED IN SOLUTION: 10°
- REFERENCE GRAVITY FIELD: GEM-7 (COMPLETE THROUGH ORDER AND DEGREE 16)
 - $R_e = 6378.745 \text{ km}$
 - $f = 1/298.255$
 - $GM = 3.986038 \times 10^5 \text{ km}^3/\text{sec}^2$
- OPERATING MODE OF ALTIMETER: GLOBAL
- STANDARD DEVIATION OF FIT: 1.4 METERS
- GROUND TRUTH SOURCE: $1^\circ \times 1^\circ$ MEAN - FREE-AIR GRAVITY ANOMALIES DMAAC.

Figure 3. Differences Between Estimated $2^\circ \times 2^\circ$ Gravity Anomalies and Ground Truth

- b) Comparing the GEOS-3 altimeter geoid with the GSFC detailed geoid (Ref. 6) (Figure 4).

The comparison of the GEOS-3 geoid with the detailed geoid for pass 1647 showed an unresolved offset of -2.4 meters and an RMS error of ± 2.2 meters along this profile.

From Figure 2(a), the RMS deviation from "ground truth" was found to be ± 9.6 mgal. The RMS error resulting from a comparison of the GEOS-3 altimeter geoid with the detailed geoid is found to be ± 2.1 meters. Using the uncertainties cited above, a simplistic relation can be constructed which says that a RMS error in a $2^\circ \times 2^\circ$ mean free air gravity anomaly of ± 4.6 mgals corresponds to uncertainty in geoidal undulation of ± 1 meter. This value closely agrees with covariance error analysis results for which ± 1 meter in geoidal undulation equals ± 5 mgals for $2^\circ \times 2^\circ$ mean free air gravity anomalies.

GEOS-3 altimetry data taken over the East Indian Ocean have been analyzed to determine gravitational features. Approximately 7200 well distributed altimeter measurements were selected from over 72,000 in 31 passes, each pass being individually fitted to the GEM-7 geoid in the region bounded by latitudes 20°S to 50°S and longitudes 90°E to 110°E . These selected measurements were used in a least squares estimation of 24 area mean free air gravity anomalies corresponding approximately to $5^\circ \times 5^\circ$ squares within the boundaries of the region (see Figure 5). The RMS error of commission for each of the estimated anomalies was found to be on the order of ± 5 mgals, varying with the data distribution within each individual block. Comparisons were made with $5^\circ \times 5^\circ$ averages of $1^\circ \times 1^\circ$ anomalies based on surface gravimetric measurements compiled by Prof. R. Rapp, Ohio State University as well as with independently estimated anomalies obtained from the analysis of satellite to satellite tracking (SST) Doppler data obtained from the Apollo-Soyuz Geodynamics Experiment of July 1975. In this comparison, most of the recovered anomalies were found to be within 6 mgals of Prof. Rapp's values with an RMS deviation of ± 9.9 mgals. For the comparison with the Apollo derived anomalies, agreement is found in all but two blocks to be within 8 mgals with an RMS of ± 7.9 mgals. Apollo derived anomalies also validate the GEOS-3 anomalies for those blocks where no "ground truth" values are available.

A local marine geoid was computed from the 24 estimated gravity anomalies and this geoid was compared along two altimeter pass profiles with the GEOS-3 altimeter sea surface height and the GSFC detailed geoid (see Figures 6-9). The two altimeter passes which are northeast to southwest (Figures 6 and 7) fit the altimeter geoid to within ± 1.5 meters, whereas the southeast to northwest passes (Figures 8 and 9) fit the altimeter geoid to within ± 3.5 meters. In the former case, the altimeter data were much less noisy than in the latter case. In addition, SE to NW passes traverse over a larger portion of a major bathy-

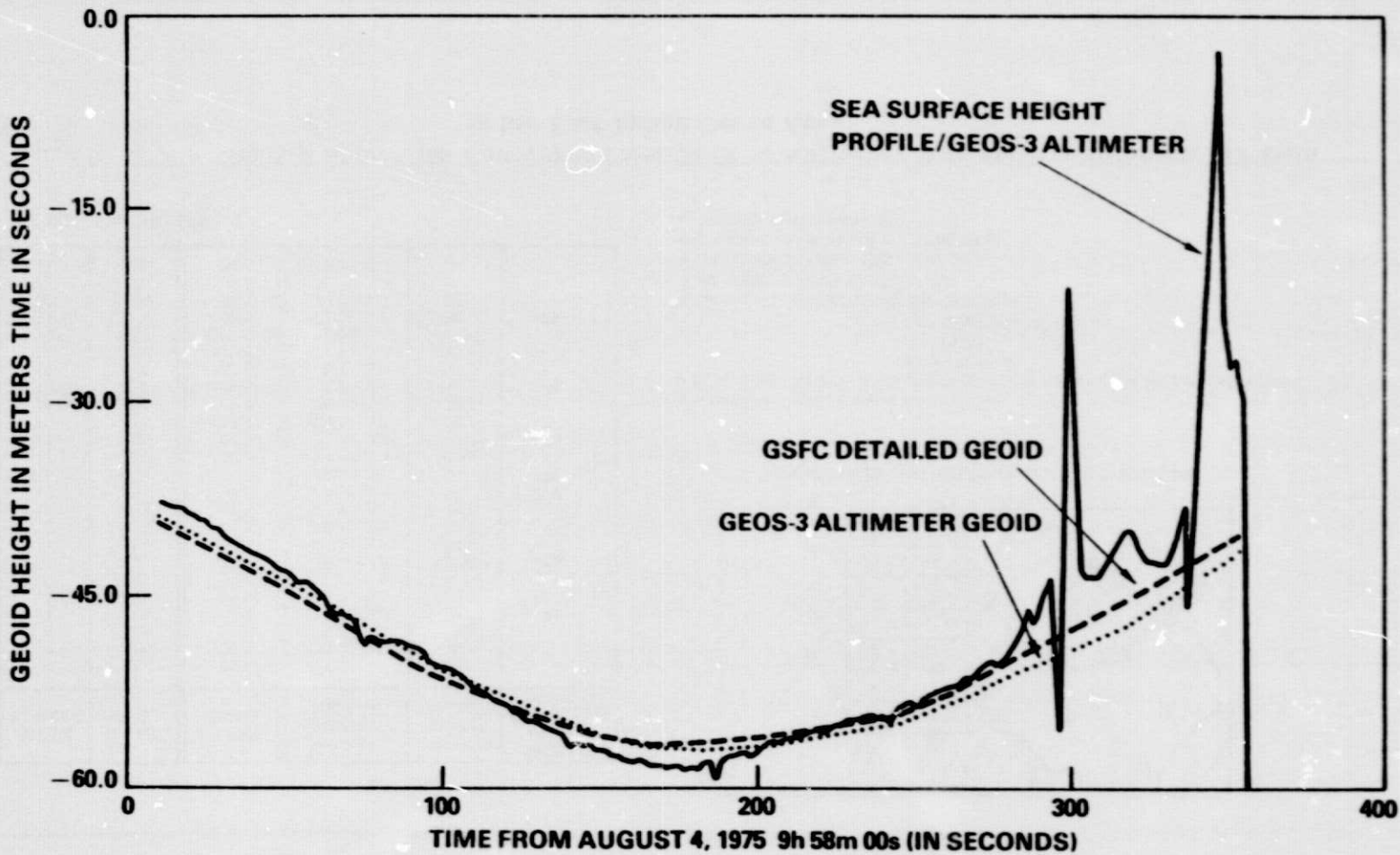
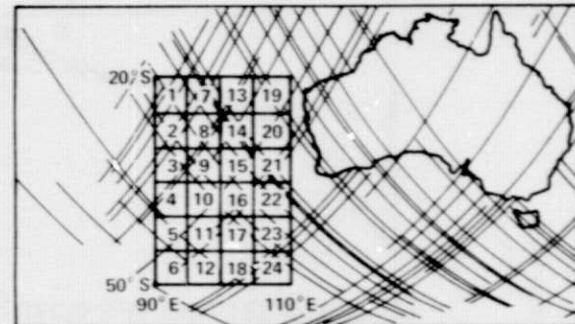


Figure 4. Comparison of GEOS-3 Altimeter Geoid with Detailed Geoid and Altimeter Sea Surface Height Profile for Revolution 1647

| BLOCK NUMBER | S. LAT. (DEG.) | E. LONG. (DEG.) | 5° x 5° ANOMALIES (MGALS) | GROUND TRUTH* (MGALS) | APOLLO 5° x 5° ANOMALIES (MGALS) |
|--------------|----------------|-----------------|---------------------------|-----------------------|----------------------------------|
| 1 | 22.5 | 92.5 | -12.7 ± 1.8 | -26.7 | |
| 2 | 27.5 | 92.5 | -19.2 ± 3.0 | -9.6 | |
| 3 | 32.5 | 92.5 | -9.0 ± 2.5 | -5.3 | |
| 4 | 37.5 | 92.5 | 0.8 ± 2.2 | -4.7 | 11 |
| 5 | 42.5 | 92.5 | -0.2 ± 4.6 | -0.7 | |
| 6 | 47.5 | 92.5 | 13.4 ± 3.8 | - | 26 |
| 7 | 22.5 | 97.5 | -19.6 ± 2.0 | -27.6 | -15 |
| 8 | 27.5 | 97.5 | -27.9 ± 3.5 | -14.0 | |
| 9 | 32.5 | 97.5 | -18.1 ± 2.3 | -22.6 | |
| 10 | 37.5 | 97.5 | -11.5 ± 6.2 | -14.6 | |
| 11 | 42.5 | 97.5 | 3.1 ± 4.9 | - | 6 |
| 12 | 47.5 | 97.5 | 10.5 ± 3.7 | - | 16 |
| 13 | 22.5 | 102.5 | -31.4 ± 3.3 | -13.6 | |
| 14 | 27.5 | 102.5 | -25.7 ± 2.2 | -7.0 | -22 |
| 15 | 32.5 | 102.5 | -23.1 ± 5.7 | -29.2 | |
| 16 | 37.5 | 102.5 | -28.1 ± 4.4 | -23.2 | |
| 17 | 42.5 | 102.5 | -7.7 ± 2.1 | - | 0 |
| 18 | 47.5 | 102.5 | -0.4 ± 5.6 | - | |
| 19 | 22.5 | 107.5 | -22.7 ± 2.9 | -13.4 | |
| 20 | 27.5 | 107.5 | -14.6 ± 5.8 | -15.5 | |
| 21 | 32.5 | 107.5 | -22.2 ± 2.5 | -36.3 | -29 |
| 22 | 37.5 | 107.5 | -27.0 ± 1.7 | -32.1 | |
| 23 | 42.5 | 107.5 | -28.7 ± 5.3 | - | |
| 24 | 47.5 | 107.5 | -9.9 ± 2.3 | - | |

*2.5 MGALS ≈ 1 METER



GROUND TRACKS OF ALTIMETER PASSES USED IN SOLUTION

- SPHERICAL DISTANCE (ψ): 10°
- REFERENCE GRAVITY FIELD: GEM-7 (COMPLETE THROUGH ORDER AND DEGREE 16)
 $R_e = 6378.145$ km
 $f = 298.255$
 $GM = 3.986008 \times 10^8 \text{ km}^3/\text{sec}^2$
- OPERATING MODE OF ALTIMETER: INTENSIVE
- NO. PASSES USED IN SOLUTION: 31
- SAMPLE RATE: 1 MEAS./SEC.
- STANDARD DEVIATION OF FIT: 15 METERS.
- GROUND TRUTH: RAPP 1976

Figure 5. 5° x 5° Gravity Anomalies Recovered from GEOS-3 Altimetry Data and Apollo/Soyuz SST Data in the East Indian Ocean Area

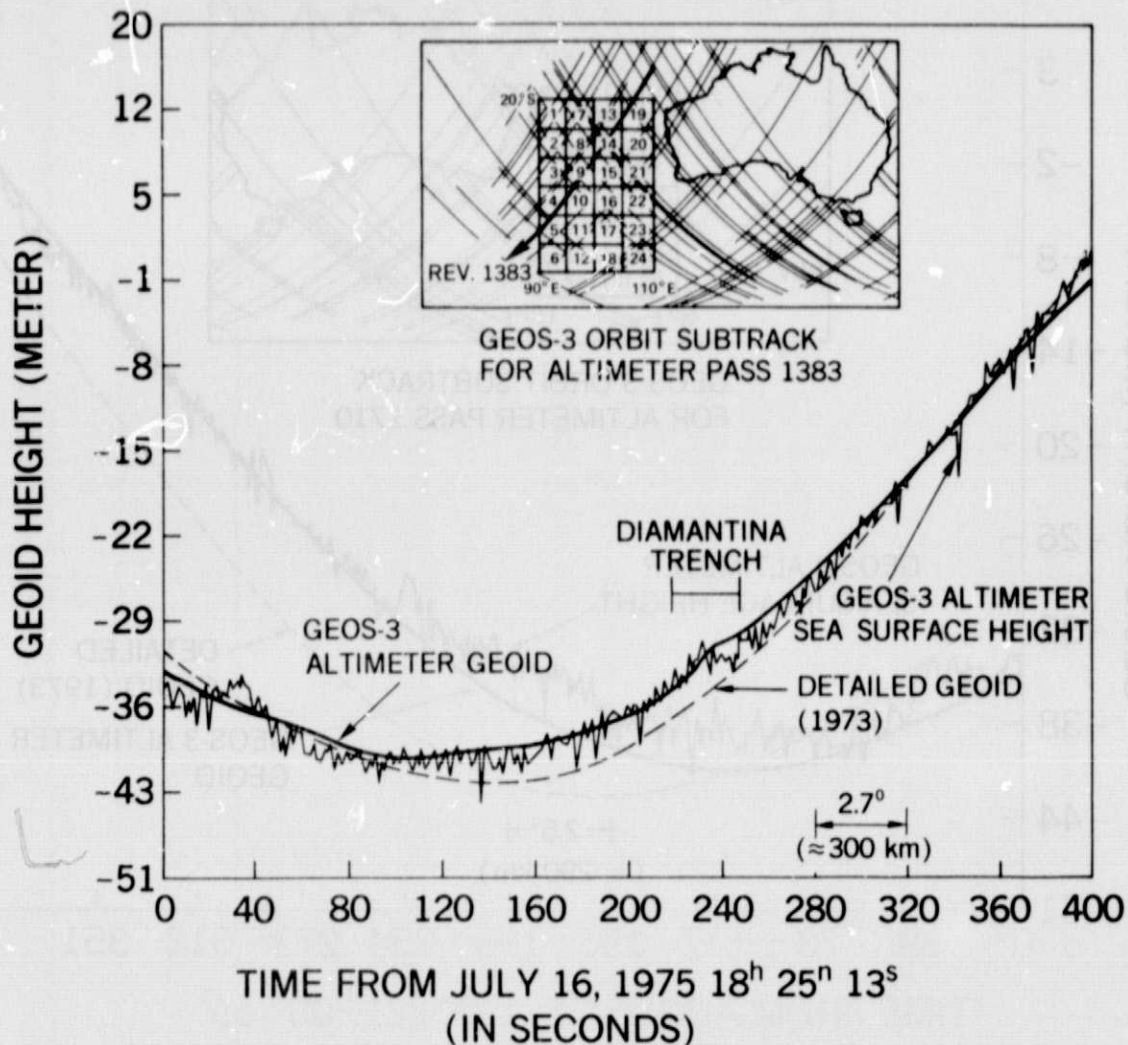


Figure 6. Comparison of GEOS-3 Altimeter Geoid with the Detailed Geoid and Sea Surface Height Profile for Revolution 1383

metric feature, the Diamantina Trench, than the NE to SW passes (see Figure 10).

CONCLUSION

The results presented in this report should be categorized as preliminary, as more attention needs to be given to seeking the best way to treat orbit errors, tides, and deviations of the instantaneous sea surface from the geoid. It is also

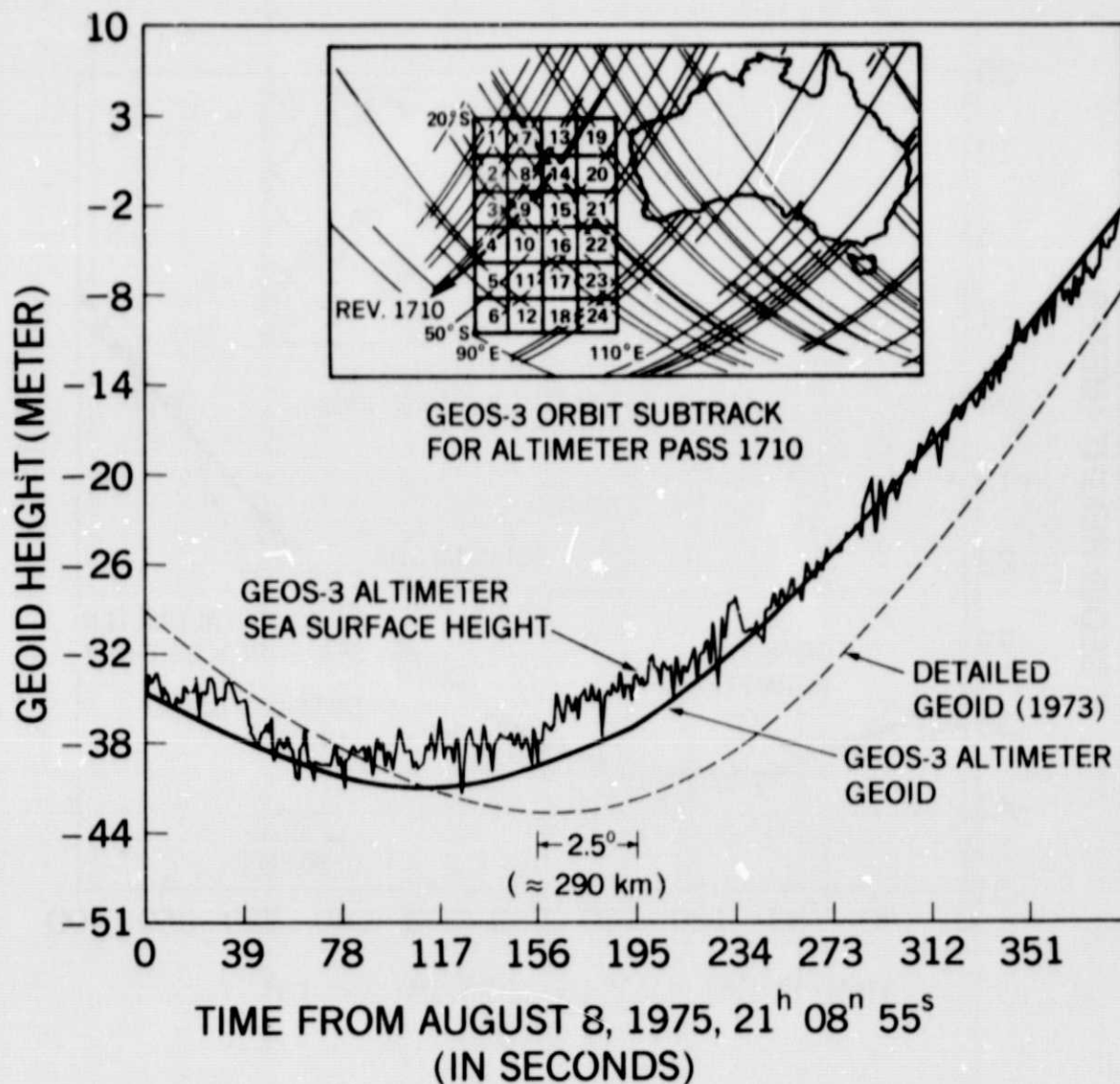
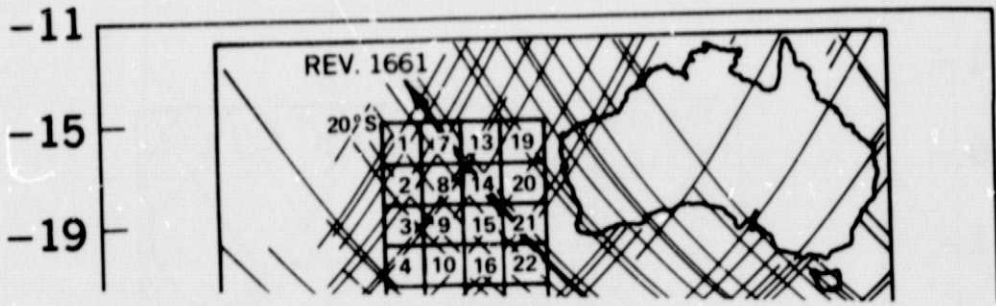


Figure 7. Comparison of GEOS-3 Altimeter Geoid with the Detailed Geoid and Sea Surface Height Profile for Revolution 1710

to be noted that the "ground truth" solutions presented here are generally not of any better quality than the altimeter solutions. Formal statistics associated with these solutions are as large or larger than those of the altimeter solution.

It can however, be concluded, that the feasibility of gravity anomaly recovery using altimeter data is proven. The altimeter data distribution available at present with the GEOS-3 satellite is sufficient for achieving $5^{\circ} \times 5^{\circ}$ anomaly block coverage over the oceans within the latitudes 65°S to 65°N .



**ORIGINAL PAGE IS
OF POOR QUALITY**

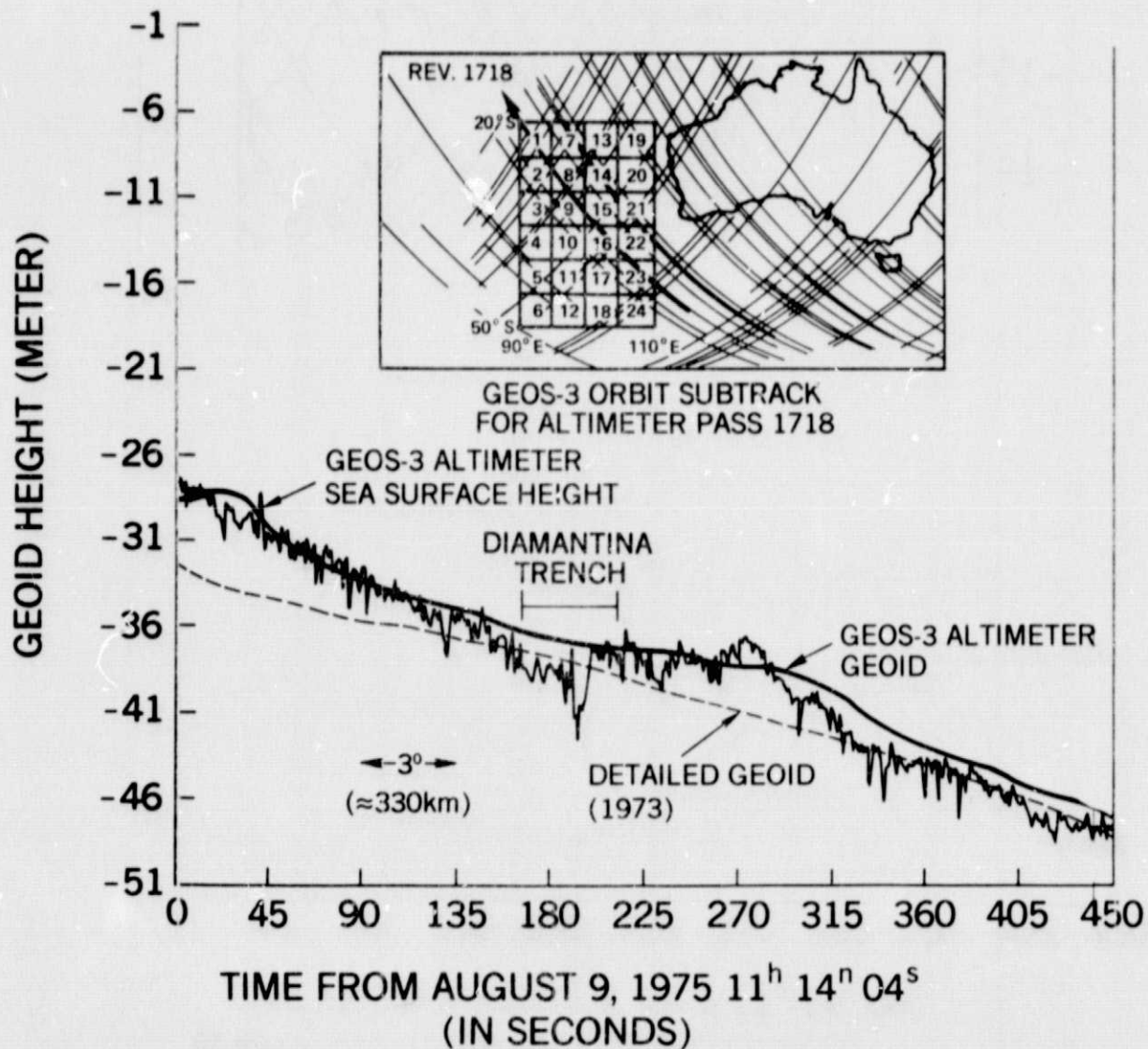


Figure 9. Comparison of GEOS-3 Altimeter Geoid with the Detailed Geoid and Sea Surface Height Profile for Revolution 1718

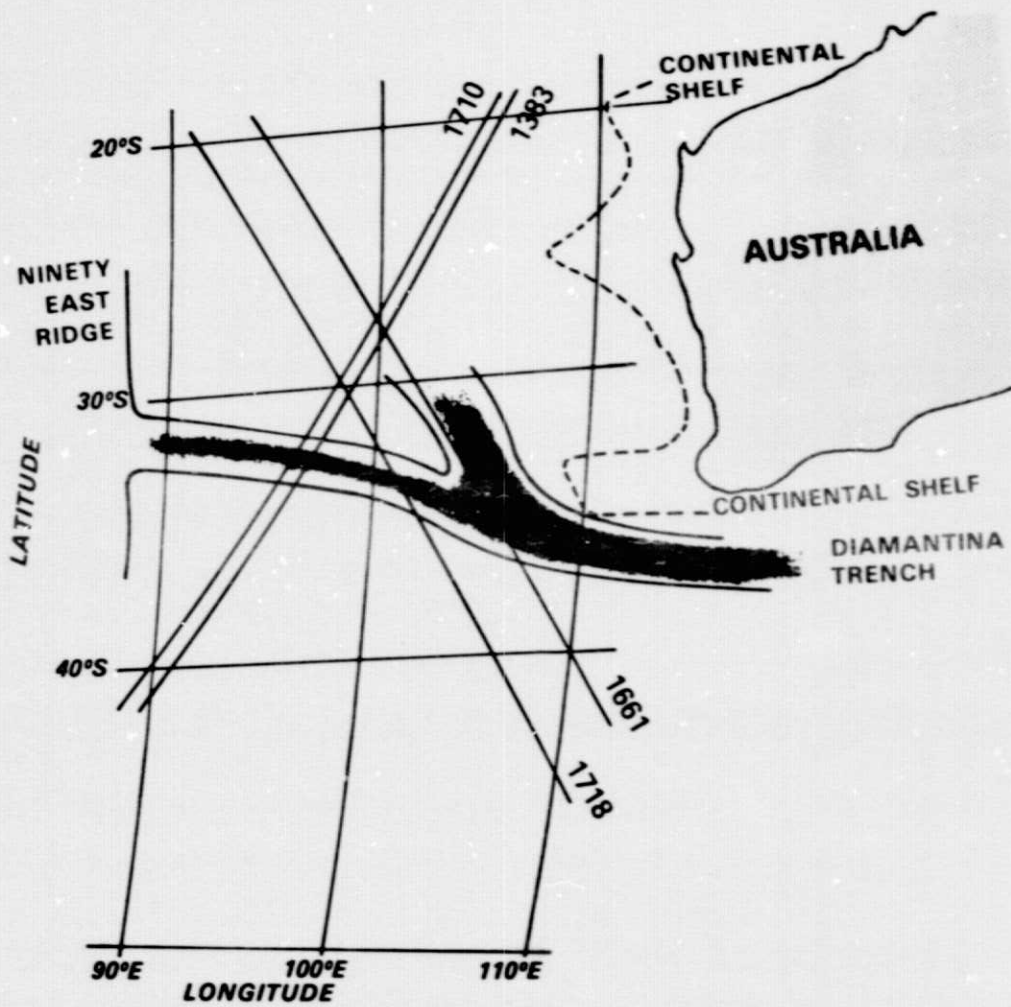


Figure 10. East Indian Ocean Area

REFERENCES

1. Vonbun, F. O., Kahn, W. D., Bryan, J. W., Schmid, P. E., Wells, W. T., Conrad, T. D., "Gravity Anomaly Detection — Apollo/Soyuz", X-926-75-308, Dec. 1975
2. Diamante, J., B. Gibbs, D. Haley, T. V. Martin, and J. R. Vetter, "GEODYN Documentation of the Mathematical Modelling for the GEOS-C Altimeter Experiment," Wolf Research and Development Corp., Document No. 001-74, Riverdale, Maryland 20840, March 1974
3. Wagner, C. A., F. J. Lerch, J. E. Brown, and J. A. Richardson, "Improvement in the Geopotential From Satellite and Surface Data (GEM-7 and -8)," NASA Goddard Space Flight Center, X-921-76-20, January 1976
4. Heiskanen, W. A., and H. Moritz, Physical Geodesy, W. H. Freeman and Co., 1967
5. Brown, R. D., "GEOS-3 Altimeter Data Noise Analysis." EOS Vol. 57, No. 12, December 1976, pp. 900 (abstract)
6. Marsh, J., and S. Vincent, A Global Detailed Geoid, NASA TM X-70492, 1973